JVI Journals.ASM.org

The Baculovirus Core Gene *ac83* Is Required for Nucleocapsid Assembly and *Per Os* Infectivity of *Autographa californica Nucleopolyhedrovirus*

Shimao Zhu, Wei Wang, Yan Wang, Meijin Yuan, Kai Yang

State Key Laboratory of Biocontrol, Sun Yat-sen University, Guangzhou, China

Autographa californica multiple nucleopolyhedrovirus **(AcMNPV)** ***ac83*** **is a baculovirus core gene whose function in the AcMNPV life cycle is unknown. In the present study, an** ***ac83*****-knockout AcMNPV (vAc83KO) was constructed to investigate the function of** ***ac83*** **through homologous recombination in** ***Escherichia coli*****. No budded virions were produced in vAc83KO-transfected Sf9 cells, although viral DNA replication was unaffected. Electron microscopy revealed that nucleocapsid assembly was aborted due to the** ***ac83*** **deletion. Domain-mapping studies revealed that the expression of Ac83 amino acid residues 451 to 600 partially rescued the ability of AcMNPV to produce infectious budded virions. Bioassays indicated that deletion of the chitin-binding domain of Ac83 resulted in the failure of oral infection of** ***Trichoplusia ni*** **larvae by AcMNPV, but AcMNPV remained infectious following intrahemocoelic injection, suggesting that the domain is involved in the binding of occlusion-derived virions to the peritrophic membrane and/or to other chitin-containing insect tissues. It has been demonstrated that Ac83 is the only component with a chitin-binding domain in the** ***per os*** **infectivity factor complex on the occlusion-derived virion envelope. Interestingly, a functional inner nuclear membrane sorting motif, which may facilitate the localization of Ac83 to the envelopes of occlusion-derived virions, was identified by immunofluorescence analysis. Taken together, these results demonstrate that Ac83 plays an important role in nucleocapsid assembly and the establishment of oral infection.**

Baculoviruses are a family of enveloped double-stranded DNA viruses that are specifically pathogenic to arthropods, mainly affecting insects of the orders Lepidoptera, Hymenoptera, and Diptera (1). Based on their whole-genome sequences, *Baculoviridae* can be divided into four genera: *Alphabaculovirus*, *Betabaculovirus*, *Gammabaculovirus*, and *Deltabaculovirus* (2). *Alphabaculovirus* encompasses lepidopteran nucleopolyhedroviruses (NPVs) and can be further subdivided into two groups, group I and group II NPVs, based on phylogenetic analysis of the *polyhedrin* (*polh*) gene (3). This grouping is coincident with the utilization of different envelope fusion proteins for spreading infection (4). *Autographa californica* multiple NPV (AcMNPV) is the best-characterized baculovirus and the first to be completely sequenced. AcMNPV has a genome of approximately 134 kbp that encodes 156 putative open reading frames (ORFs) (5). To date, 59 baculovirus genomes have been completely sequenced, and these genomes have 37 core genes in common (1, 6, 7).

A unique feature during the life cycle of a baculovirus is the production of two morphologically distinct but genetically identical progeny virion phenotypes, budded virions (BVs) and occlusion-derived virions (ODVs). BVs are produced early in infection. Nucleocapsids assemble in the nucleus, migrate through the cytoplasm, and bud out of the plasma membrane to form BVs. BVs are able to spread infections within infected insect tissues and are responsible for establishing systemic infection. During the late phase of infection, nucleocapsids are retained in the nucleus and are enveloped by the virus-induced intranuclear microvesicles to form ODVs. ODVs are subsequently occluded within a proteinaceous crystal matrix to form occlusion bodies (OBs).

Although the nucleocapsids of BVs and ODVs are similar, their major differences are reflected in the composition of their envelopes, which accommodate their distinct roles (8, 9). Baculoviruses initiate infection when their insect hosts orally consume OB-contaminated food. A number of ODV envelope proteins, designated *per os* infectivity factors (PIFs), play roles in oral infectivity. Currently, seven PIFs have been identified: P74 (PIF0), PIF1, PIF2, PIF3, PIF4, PIF5, and PIF6 (10–16). All the PIF genes are baculovirus core genes (17), indicating that the *per os* infection processes have been conserved during evolution. Recently, the *Spodoptera frugiperda* NPV ORF58 (Sf58), which is conserved only in lepidopteran baculoviruses and is homologous to Ac108 in AcMNPV, was shown to be a PIF (18). Proteomic mass spectrometric analysis revealed that at least six proteins, P74, PIF1, PIF2, PIF3, PIF4, and Ac83, together with three other potential components, Ac5, PIF6, and Ac108, are present as a complex on the ODV envelope (19). PIF1, PIF2, and PIF3 form a stable core. PIF4 interacts strongly with the core, whereas P74 and Ac83 interact loosely with it (19).

Ac83 is encoded by the baculovirus core gene *ac83*. Sequence analysis revealed that homologs of Ac83 from *Alphabaculovirus* and *Gammabaculovirus* contain a type II chitin-binding domain (CBD) at the N terminus (20). The type II CBD is characterized by the presence of a 6-cysteine motif with the consensus sequence C-$X_{13–20}$-C-$X_{5–6}$-C-$X_{9–19}$-C-$X_{10–14}$-C-$X_{4–14}$-C (where X is any amino acid other than cysteine) (21). The type II CBD is also referred to as the peritrophin-A domain because it is found in peritrophin-A chitin-binding proteins, particularly in the peritrophins of insect peritrophic membranes (PM) (21). In addition,

Received 3 May 2013 **Accepted** 11 July 2013
Published ahead of print 17 July 2013
Address correspondence to Kai Yang, yangkai@mail.sysu.edu.cn.

doi:10.1128/JVI.01207-13

type II CBDs have also been identified in proteins from the ecdysozoan clade that are frequently involved in the interaction with chitin (21, 22).

As the only component with a CBD in the PIF complex, it is thought that Ac83 plays a role in the oral infectivity of ODVs, but such a role has never been confirmed (19). *ac83* encodes a putative protein of 847 amino acids (aa) with a predicted molecular mass of approximately 96 kDa (5). Proteomic analyses of the protein compositions of the BVs and ODVs of AcMNPV suggest that Ac83 is associated only with the ODV envelope (23, 24). However, the Ac83 homolog in *Orgyia pseudotsugata* NPV, OpP91, has been observed to localize predominantly to the capsid structure in BVs and ODVs (25). The closely related *ac83* homolog in *Bombyx mori* NPV, *BmP95*, has been shown to be essential for nucleocapsid assembly, and deletion of *BmP95* led to a defect in the spreading of the infection in cultured cells (20, 26).

In this study, an *ac83*-knockout virus was constructed in order to investigate the role of *ac83* in the AcMNPV life cycle. We demonstrated that deletion of *ac83* resulted in the failure of nucleocapsid assembly and of the subsequent morphogenesis of progeny BVs and ODVs. The rescue of Ac83 amino acid residues 451 to 600, which make up only approximately one-fifth of the full-length Ac83 protein (847 aa), was sufficient to produce infectious BVs. Most importantly, we observed that the CBD of Ac83 was essential for the establishment of efficient *per os* infection by AcMNPV. Considering the ubiquitous presence of chitin in the PM and the microvilli of epithelial cells of the insect midgut, and given that Ac83 is the only known component with a CBD in the PIF complex (19), we suggest that the CBD of Ac83 may assist in initiating primary viral infection by enhancing the binding of ODVs to the chitin components associated with the PM or microvilli.

MATERIALS AND METHODS

Bioinformatic analyses. The homologs of Ac83 were searched against the nonredundant protein sequences at the NCBI database (http://blast.ncbi.nlm.nih.gov/Blast.cgi?PROGRAM=blastp&BLAST_PROGRAMS=blastp&PAGE_TYPE=BlastSearch&SHOW_DEFAULTS=on&LINK_LOC=blasthome) with the position-specific iterated (PSI) BLAST algorithm. The conserved domains of Ac83 were predicted from the UniProt database (http://www.uniprot.org/uniprot/Q06670), the NCBI Conserved Domain Search database (http://www.ncbi.nlm.nih.gov/Structure/cdd/wrpsb.cgi) (27), SMART (28), and HHpred (29). Multiple sequence alignments were constructed using Clustal X (30) with default settings and were edited with GeneDoc (31).

Viruses and cell lines. The bacmid bMON14272 (Invitrogen), which contains an AcMNPV genome, was maintained in DH10B cells as described previously (32). Sf9 (*Spodoptera frugiperda* IPLB-Sf21-AE clonal isolate 9) insect cells were cultured at 27°C in TNM-FH medium (Invitrogen) supplemented with 10% fetal bovine serum (Invitrogen), penicillin (100 μg/ml), and streptomycin (30 μg/ml). The titers of BVs were determined by a 50% tissue culture infective dose ($TCID_{50}$) endpoint dilution assay in Sf9 cells as described previously (33). The viral inoculum was allowed to adsorb to cells for 1 h of infection or 5 h of transfection at 27°C and was then replaced with fresh medium. Time zero was defined as the time when the viral inoculum was replaced.

Transcriptional analysis of *ac83* and rapid amplification of 5′ cDNA ends (5′ RACE). Sf9 cells (1×10^6) either were mock infected or were infected with AcMNPV at a multiplicity of infection (MOI) of 5 $TCID_{50}$s/cell. The cells were collected at different hours postinfection (p.i.). Total RNA was extracted using an RNeasy Mini Kit (Qiagen) and was quantified by optical density measurements at 260 nm. After the RNA samples were treated with RNase-Free DNase (Promega), the first strand of cDNA was synthesized using an iScript cDNA synthesis kit (Bio-Rad). Reverse transcription-PCR (RT-PCR) with the *ac83*-specific primer pair ac83504/ac83304 was used to detect the *ac83* transcripts. All PCR primers are listed in Table 1.

5′ RACE analysis was performed to map the transcription start site of *ac83*. The *ac83*-specific reverse primers ac83305 and ac83306, together with the adaptor primers provided in the 5′/3′ RACE Kit, 2nd Generation (Roche), were used for PCR amplification, and 1 μg of purified total RNA isolated from the AcMNPV-infected Sf9 cells at 24 h p.i. was used as the template. The PCR products were purified with a gel extraction kit (Omega) and were cloned into the pMD18-T vector (TaKaRa) for sequencing.

Time course analysis of Ac83 synthesis. Sf9 cells (1×10^6) were infected with vAc83:HA (a recombinant AcMNPV in which Ac83 was tagged with a hemagglutinin [HA] epitope; see details below) at an MOI of 10 $TCID_{50}$s/cell. At the designated time points p.i., cells were scraped, collected, and centrifuged at 3,000 × *g* for 5 min at room temperature. Western blotting was performed using a mouse monoclonal anti-HA antibody (1:3,000; Abcam) as the primary antibody and a horseradish peroxidase (HRP)-conjugated goat anti-mouse antibody (1:5,000; Amersham Biosciences) as the secondary antibody to detect the expression profile of Ac83.

Generation of an *ac83*-knockout AcMNPV bacmid. An *ac83*-knockout AcMNPV bacmid, designated bAc83KO, was generated as described previously, using primer pairs ac83502/ac83302 and ac83503/ac83303 (34). To avoid affecting adjacent genes, 360 nucleotides (nt) from the 5′ region of the *ac83* ORF (AcMNPV nt 67884 to 68243) and 127 nt from the 3′ region of the *ac83* ORF (AcMNPV nt 70301 to 70427) were preserved.

Construction of an *ac83*-knockout virus. To facilitate the examination of viral infection, the AcMNPV *polh* and *enhanced green fluorescence protein* (*egfp*; referred to as *gfp* in this study) genes were inserted into the *polh* locus of bAc83KO to generate the *ac83*-knockout virus $vAc^{ac83KO\text{-}PH\text{-}GFP}$ (vAc83KO) as described previously (35). A wild-type control virus, $vAc^{WT\text{-}PH\text{-}GFP}$ (vAcWT), was generated by the insertion of *polh* and *gfp* into bMON14272.

To generate an *ac83*-repaired virus, the donor plasmid pFB1-Ac83:HA-PG was constructed as follows. A 2,984-bp fragment containing an *ac83* native promoter and the *ac83* ORF tagged with an HA epitope prior to the *ac83* stop codon (Ac83POHA) was PCR amplified using bMON14272 as the template and ac83501 and ac83301 as the primers. The PCR product was ligated into pUC18-SV40 (36) to generate pUC18-Ac83:HA. pUC18-Ac83:HA was subsequently digested with EcoRI and XbaI, and the resulting Ac83:HA fragment was ligated into pFB1-PH-GFP (34) to generate the donor plasmid pFB1-Ac83:HA-PG. Electrocompetent DH10B cells containing the helper plasmid pMON7124 and bAc83KO were transformed with pFB1-Ac83:HA-PG to generate the *ac83*-repaired virus $vAc^{ac83REP\text{-}HA\text{-}PH\text{-}GFP}$ (vAc83:HA).

Construction of different truncated forms of *ac83* rescue viruses. A set of recombinant AcMNPVs with different *ac83* gene truncations was generated to investigate the portion of Ac83 that is important for viral replication. The overlap PCR technique was used to construct the truncated Ac83 protein variants as described previously (37). Briefly, to delete the predicted inner nuclear membrane sorting motif (INM-SM) of Ac83, primers ac83501/ac83307 and ac83505/ac83301 were used to amplify the upper and lower overlap fragments of *ac83*, respectively, from pFB1-Ac83:HA-PG. Overlap PCR was conducted by mixing the resulting PCR products with the outmost primers ac83501 and ac83301. In the same manner, with primers ac83501/ac83308 and ac83506/ac83301, the predicted CBD of Ac83 was deleted, and the predicted proline-rich (PR) region of Ac83 was deleted using primers ac83501/ac83309 and ac83507/ac83301. To delete aa 2 to 290 (numbering is from the N terminus of Ac83 in this paper) from Ac83, primers ac83501/ac83310 and ac83508/ac83301 were used, while primers ac83501/ac83311 and ac83509/ac83301 were used for the deletion of Ac83 aa 2 to 450. The *ac83* gene-specific primer ac83501 was used in combination

TABLE 1 Primer sequences used in this study

Application	Primer	Sequence
Amplification of *ac83* flanking sequences	ac83502	5′-GAGCTCATGATGTCTGGCGTAATGTTGCTC-3′
	ac83302	5′-GGATCCGTTGGGATTTTCATCATTTGCTCTA-3′
	ac83503	5′-CTGCAGGCACGTCAAAAACGGCCAATAC-3′
	ac83303	5′-AAGCTTCTTTACGAGTAGAATTCTACTTGTAAAACATAATC-3′
Amplification of *ac83* promoter	ac83501	5′-GAATTCGCTCATCGATAGCGGCGGCGGA-3′
Amplification of the 3′ end of *ac83* tagged with HA	ac83301	5′-GGATCCTTAGGCGTAATCTGGGACGTCGTATGGGTATACAATGGAATCTTCTTGT AAATTATCCAA-3′
Reverse transcription analysis of *ac83*	ac83504	5′-CAAGCTAACCAGTTGTCATGCGGAA-3′
	ac83304	5′-TTATACAATGGAATCTTCTTGTAAATTATCC-3′
5′ RACE analysis of *ac83*	ac83305	5′-CACGGGAACACATTTTAGTTGTGCGTA-3′
	ac83306	5′-GTCGCCGCTCAAAATAAACTCG-3′
Deletion of Ac83 INM-SM	ac83307	5′-TATTCAGTCATCACTTGCATCGTGAACGCCCAAATCA-3′
	ac83505	5′-GGCGTTCACGATGCAAGTGATGACTGAATATGTGAAG-3′
Deletion of Ac83 CBD	ac83308	5′-GTGTCCGGCGCCGTTAACTTTACACTGGCCGGTTTC-3′
	ac83506	5′-GGCCAGTGTAAAGTTAACGGCGCCGGACACACGTAC-3′
Deletion of Ac83 PR region	ac83309	5′-ATAAAATAAATCTTTGTTGTCTAATATTAGCGCCACTACCCAATGGTCG-3′
	ac83507	5′-CTAATATTAGACAACAAAGATTTATTTTATTCATG-3′
Deletion of Ac83 aa 2–290	ac83310	5′-CGATATCGGCCGTCATCGTGAACGCCCAAATCA-3′
	ac83508	5′-GCGTTCACGATGACGGCCGATATCGGCGAC-3′
Deletion of Ac83 aa 2–450	ac83311	5′-GGCGTCGTTGTTTAACATCGTGAACGCCCAAATCA-3′
	ac83509	5′-TGGGCGTTCACGATGTTAAACAACGACGCCATCTTTG-3′
Deletion of Ac83 aa 742–847	ac83312	5′-GGATCCTTAGGCGTAATCTGGGACGTCGTATGGGTATTTAACGTTGTTGCGTAACTCGT-3′
Deletion of Ac83 aa 601–847	ac83313	5′-GGATCCTTAGGCGTAATCTGGGACGTCGTATGGGTATTTGGGCCGTTTTACGAGAG-3′
Deletion of Ac83 aa 551–847	ac83314	5′-GGATCCTTAGGCGTAATCTGGGACGTCGTATGGGTATTCGTTTTCTACGATTTTTTGG-3′
Amplification of Ac83 INM-SM	ac83510	5′-GGATCCATGATGTCTGGCGTAATGTTGCTC-3′
	ac83316	5′-GAATTCAGTCATCACTTGGAGCCGCTTG-3′
Amplification of *gfp*	GFP-F	5′-GAATTCATGGGCAAAGGAGAAGAACTTTTCACTG-3′
	GFP-R	5′-TCTAGATTATTTGTATAGTTCATCCATGCCATG-3′
Real-time PCR specific for AcMNPV DNA	gp41-F	5′-CGTAGTGGTAGTAATCGCCGC-3′
	gp41-R	5′-AGTCGAGTCGCGTCGCTTT-3′

with the *ac83* gene truncation-specific primers ac83312, ac83313, and ac83314 to generate C-terminally truncated Ac83 protein variants. Finally, Ac83 aa 2 to 450 and aa 601 to 847 were deleted from Ac83 using primers ac83501 and ac83313, and the Ac83:del2-450 fragment was used as the template. The PCR products were cloned between EcoRI and BamHI sites in pUC18-SV40, and the resulting constructs were digested with EcoRI and XbaI and were ligated into the donor plasmid pFB1-PH-GFP. Electrocompetent DH10B cells containing the pMON7124 helper plasmid and the bAc83KO bacmid were transformed with the donor plasmids mentioned above to generate different truncated forms of the *ac83* rescue viruses: vAc$^{ac83REP\text{-}delINM\text{-}SM\text{-}PH\text{-}GFP}$ (vAc83:delSM), vAc$^{ac83REP\text{-}delCBD\text{-}PH\text{-}GFP}$ (vAc83:delCBD), vAc$^{ac83REP\text{-}delPR\text{-}PH\text{-}GFP}$ (vAc83:delPR), vAc$^{ac83REP\text{-}del2\text{-}290\text{-}PH\text{-}GFP}$ (vAc83:del2-290), vAc$^{ac83REP\text{-}del2\text{-}450\text{-}PH\text{-}GFP}$ (vAc83:del2-450), vAc$^{ac83REP\text{-}del742\text{-}847\text{-}PH\text{-}GFP}$ (vAc83:del742-847), vAc$^{ac83REP\text{-}del601\text{-}847\text{-}PH\text{-}GFP}$ (vAc83:del601-847), vAc$^{ac83REP\text{-}del551\text{-}847\text{-}PH\text{-}GFP}$ (vAc83:del551-847), and vAc$^{ac83REP\text{-}del2\text{-}450/601\text{-}847\text{-}PH\text{-}GFP}$ (vAc83:del2-450/601-847).

Time course analysis of BV production. Sf9 cells (1×10^6) either were transfected in triplicate with 1.0 μg of bacmid DNA using Cellfectin liposome reagent (Invitrogen) or were infected with the indicated viruses at an MOI of 0.1 $TCID_{50}$/cell. At the designated time points posttransfection (p.t.) or p.i., the supernatants containing BVs were harvested, and the titers were determined in duplicate using a $TCID_{50}$ endpoint dilution assay (33). To determine whether any noninfectious BVs were produced in vAc83KO-transfected cells, the supernatants and cell pellets were harvested at 72 h p.t. for Western blotting as described previously (35). A polyclonal primary antibody against AcMNPV VP39 (dilution, 1:3,000) (38) was used to detect the presence of the major capsid protein VP39.

Analysis of viral DNA synthesis by qPCR. To evaluate any effect of *ac83* deletion on viral DNA replication, quantitative real-time PCR (qPCR) analysis was performed as described previously (6).

Electron microscopy analysis. Sf9 cells (1×10^6) were either transfected with 1 μg of bacmid DNA or infected with virus at an MOI of 5 $TCID_{50}$s/cell. At 72 h p.t. or 60 h p.i., the cells were collected and were prepared for electron microscopy as described previously (6). The samples were examined with a JEOL JEM-1400 transmission electron microscope at an accelerating voltage of 120 kV.

***In vivo* infectivity assays.** The infectivity of BVs *in vivo* was examined by hemocoelically injecting different doses of BVs of vAcWT, vAc83:HA, or vAc83:delCBD into 4th-instar *Trichoplusia ni* larvae. H_2O was used as a blank control. For the oral infectivity bioassays, OBs of vAcWT, vAc83:HA, or vAc83:delCBD purified from infected Sf9 cells were administered to newly molted 4th-instar *T. ni* larvae via oral inoculation as described previously (13). To destroy the PM in the midgut, newly molted 4th-instar *T. ni* larvae were treated with calcofluor white as described previously (39). A cohort of 24 larvae was used for each treatment, and the treatment was repeated in triplicate. At 24 h postinoculation, fresh diet was provided to the larvae except when the diet had not been entirely consumed. Infected larvae were reared individually in 24-well plates and were monitored daily until all larvae had either pupated or died. The data were analyzed by one-way analysis of variance (ANOVA) followed by Tukey's test.

BV and ODV purification. BVs and ODVs were purified, and ODVs were fractionated into envelopes and nucleocapsids, as described previously (6). Immunoblotting was performed as described above with a monoclonal anti-HA antibody or one of the following primary antibodies: (i) a polyclonal antibody against AcMNPV ODV-E25 (dilution, 1:2,000) (24) or (ii) a polyclonal antibody against AcMNPV VP39. An HRP-conjugated goat anti-rabbit antibody (1:8,000; Amersham Biosciences) or an HRP-conjugated goat anti-mouse antibody was used as the secondary antibody.

Generation of a transient expression plasmid expressing INM-SM-GFP and a recombinant virus hyperexpressing INM-SM-GFP. To investigate whether the INM-SM of Ac83 is functional, a transient expression assay was performed. A *gfp* gene was PCR amplified from pFB1-PH-GFP using primers GFP-F and GFP-R. The PCR product was digested with EcoRI and XbaI and was inserted into pIB/V5-His (Invitrogen) to generate pIB-GFP. The INM-SM of Ac83 was PCR amplified from bMON14272 using primers ac83510 and ac83316. The PCR product was digested with BamHI and EcoRI and was ligated into pIB-GFP to construct pIB-SM-GFP.

To generate a recombinant virus expressing green fluorescent protein (GFP) in frame with the Ac83 INM-SM under the control of the *polh* promoter, pIB-SM-GFP was digested with BamHI and XbaI, and the resulting fragment was inserted into pFastBac1 (Invitrogen) to generate donor plasmid pFB1-SM-GFP. The site-specific transposition of INM-SM-GFP into bMON14272 was performed as described above. The recombination of the resulting virus, vAcSM-GFP, in which INM-SM-GFP was placed under the control of the *polh* promoter for hyperexpression, was confirmed by PCR analysis.

Immunofluorescence. Immunofluorescence analysis was performed as described previously (6). Cells were directly stained with 4′,6-diamidino-2-phenylindole (DAPI; Roche) to detect the distribution of DNA. GFP fluorescence and the immunofluorescence of HA were examined using a Leica TCS SP5 laser scanning confocal microscope with the same parameter settings as those used for the mock-infected cells in each experiment.

RESULTS

Evolutionary conservation of Ac83 domains. The full-length Ac83 amino acid sequence was used as a query to scan the UniProt catalog, the NCBI Conserved Domain Search database, and the SMART server. In addition, the amino acid sequences of Ac83 homologs were aligned in order to analyze their evolutionary conservation. In summary, all Ac83 homologs contained the Baculo_VP91_N domain (aa 22 to 192) and a transmembrane domain (TM) at the N terminus (aa 5 to 27). A typical type II CBD (aa 224 to 282) was highly conserved in all Ac83 homologs from NPVs but was weakly conserved in granulosis viruses (GVs) (Fig. 1). The CBD domain could be predicted in two Ac83 homologs of GVs (*Cydia pomonella* GV and *Cryptophlebia leucotreta* GV) by UniProt but not by NCBI, although sequence alignment showed that the CBD domains predicted in the Ac83 homologs of these two GVs were profoundly diversified (Fig. 1). In addition, a PR region (aa 671 to 698) was present in the Ac83 homologs from group I NPVs and some group II NPVs but was absent from Ac83 homologs of the lepidopteran GVs and Hymenoptera and Diptera NPVs (Fig. 1).

After careful inspection, we hypothesized that a putative C2HC-type zinc finger (aa 148 to 197) with the consensus sequence C-X_5-C-X_n-H-X_6-C (where X is any amino acid) was present in the N-terminal regions of all the Ac83 homologs (Fig. 1). In agreement with our prediction, it has been suggested previously that BmP95 possesses two putative zinc fingers in its N terminus (40). Since the zinc finger motif has been observed to be widely involved in protein-DNA and protein-protein interactions (41, 42), its presence in Ac83 homologs may suggest a role for the Ac83 homologs in the interaction with viral DNA or other proteins.

***ac83* is a late gene.** The temporal transcriptional pattern of *ac83* was determined by RT-PCR using the total RNA extracted from AcMNPV-infected Sf9 cells at various time points p.i. As shown in Fig. 2A, *ac83* transcripts were first detected at 24 h p.i. and remained detectable up to 48 h p.i. *pe38* was used to represent baculovirus early genes, and *vp39* was used as a late gene. As expected, *pe38* transcripts were first detected at 3 h p.i., and *vp39* transcripts were first detected at 24 h p.i. (data not shown). No signals could be detected in mock-infected cells or by using the templates without reverse transcription prior to PCR, indicating that there was no contamination of genomic DNA in the RT-PCR analysis (data not shown).

Sequence analysis of the 300 nt upstream of the predicted start codon of the *ac83* ORF (ATG) indicated that there were two canonical baculovirus late gene promoter motif TAAG elements located at nucleotide positions −215 and −70 and four early baculovirus promoter motifs, CAGT or CATT, located at nucleotide positions −265, −234, −226, and −218. To determine the transcription initiation site of *ac83*, 5′ RACE analysis was performed using the total RNA isolated from AcMNPV-infected cells at 24 h p.i. Three clones derived from the 5′ RACE products were sequenced, and the results indicated that the transcription of *ac83* was initiated at the first A of the proximal canonical baculovirus late gene promoter motif TAAG (nt −69) (Fig. 2C). This agrees with the data on *ac83* from another study (43).

To determine the time course of Ac83 expression in virus-infected cells, vAc83:HA-infected Sf9 cells were collected at the time points p.i. indicated in Fig. 2B and were analyzed by immunoblotting with a monoclonal anti-HA antibody. An immunoreactive band of approximately 115 kDa, larger than the predicted molecular mass of Ac83 (96 kDa), was first observed at 24 h p.i. and persisted at 96 h p.i. (Fig. 2B). The expression profile of Ac83 was similar to that of the baculovirus late gene *vp39* (data not shown). Thus, these results demonstrated that *ac83* is a baculovirus late gene.

Construction of an *ac83*-knockout AcMNPV. To investigate the role of Ac83 in the baculovirus life cycle, the AcMNPV bacmid bMON14272 was used to replace a 2,057-bp region of *ac83* with a 1,038-bp *Cm* cassette via the λ Red recombination system as described previously (6). In the resulting *ac83*-knockout bacmid (named bAc83KO), the expression of *ac83* was thought to be completely disrupted. In addition, 360 nt from the 5′ end and 127 nt from the 3′ end of the *ac83* ORF were retained to preserve the putative promoter of *ac82* and homologous region 3 (Fig. 3A).

To examine whether the deletion of *ac83* had any effects on OB morphogenesis and to facilitate the observation of the progress of viral infection, an *ac83*-knockout AcMNPV, named vAc83KO, was constructed by inserting the *polh* gene of AcMNPV and the *gfp* gene into the *polh* locus of bAc83KO via Tn*7*-mediated transposition as described previously (34). Similarly, the two genes were inserted into bMON14272 to generate a wild-type AcMNPV control, named vAcWT. To confirm the phenotype resulting from the deletion of *ac83*, an HA tag prior to the *ac83* stop codon was inserted, together with the two genes, into bAc83KO to generate a rescue virus, named vAc83:HA (Fig. 3A).

***ac83* is essential for BV production.** To determine the effect of *ac83* deletion on viral replication, Sf9 cells were transfected with vAc83KO, vAc83:HA, or vAcWT, and the infection was monitored using fluorescence microscopy. No obvious differences in the number of fluorescent cells were observed between these viruses at 24 h p.t., indicating comparable transfection efficiencies of approximately 20% (Fig. 3B). By 72 h p.t., nearly all cells transfected with vAcWT or vAc83:HA displayed fluorescence. However, the number of vAc83KO-transfected cells displaying fluorescence did not increase from 24 to 72 h p.t. (Fig. 3B). Light

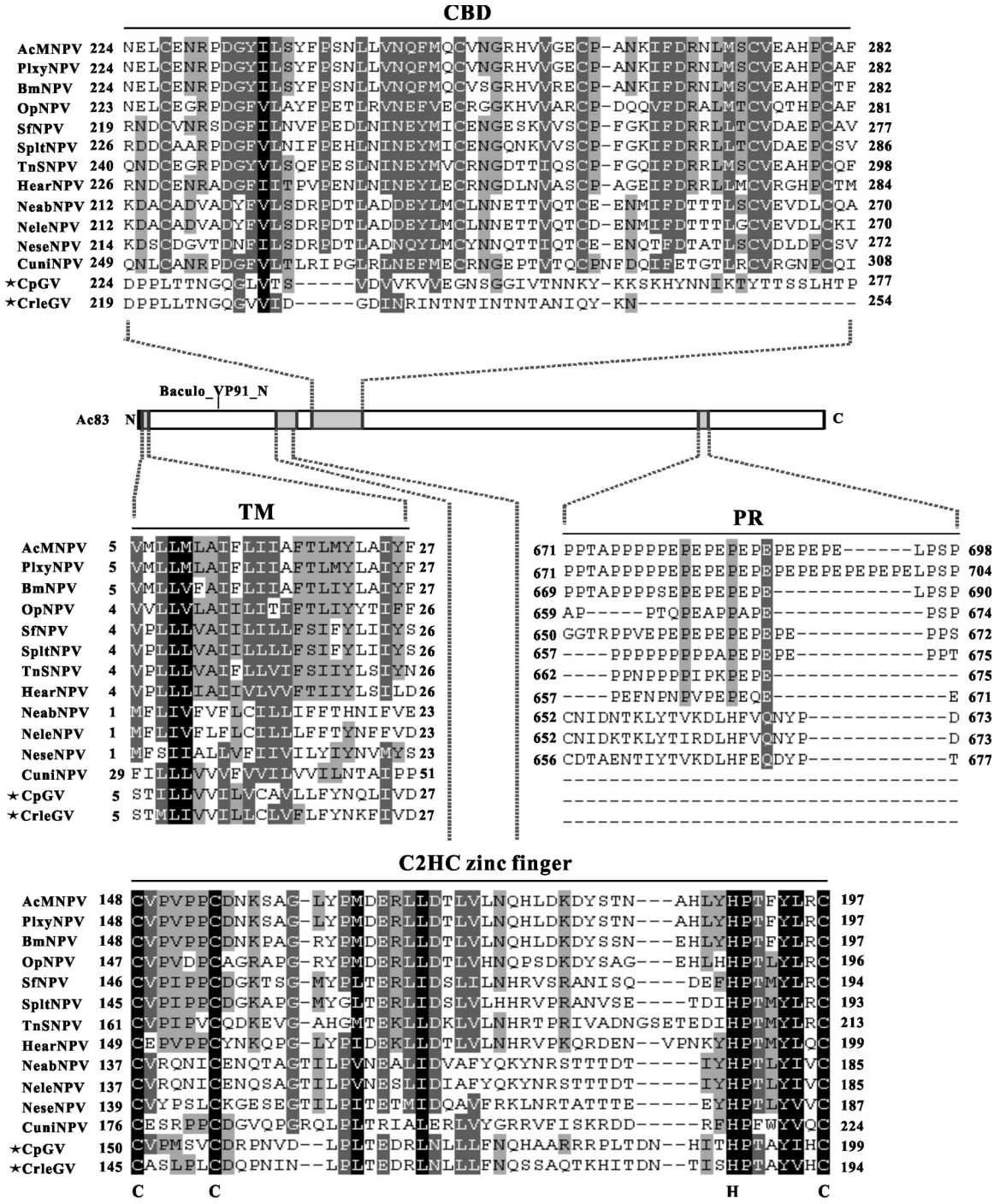

FIG 1 Overview of the conservation of Ac83 domains. The predicted domains of Ac83 are indicated in the scheme. Alignments of the CBD, TM, PR, and putative C2HC zinc finger regions of Ac83 homologs are shown. The Ac83 homologs of GVs are marked with asterisks. The cysteine and histidine residues that define the C2HC zinc finger are shown below the alignment. Black shading denotes 100% conservation. Dark gray and light gray shading represent 80 and 60% conservation, respectively. The alignment was performed using ClustalX and was edited with GeneDoc software. PlxyNPV, *Plutella xylostella* NPV; BmNPV, *Bombyx mori* NPV; OpNPV, *Orgyia pseudotsugata* NPV; SfNPV, *Spodoptera frugiperda* NPV; SpltNPV, *Spodoptera litura* NPV; TnSNPV, *Trichoplusia ni* single NPV; HearNPV, *Helicoverpa armigera* NPV; NeabNPV, *Neodiprion abietis* NPV; NeleNPV, *Neodiprion lecontei* NPV; NeseNPV, *Neodiprion sertifer* NPV; CuniNPV, *Culex nigripalpus* NPV; CpGV, *Cydia pomonella* GV; CrleGV, *Cryptophlebia leucotreta* GV.

microscopy revealed no differences in OB formation in any of the three viruses up to 48 h p.t. However, by 96 h p.t., most of the cells transfected with vAcWT or vAc83:HA contained OBs, whereas the number of vAc83KO-transfected cells containing OBs did not increase (Fig. 3B). These results suggested that *ac83* is essential for the production of infectious BVs. The deletion of *ac83* did not affect the progression of infection into the very late phase, as evidenced by the formation of OBs in vAc83KO-transfected cells.

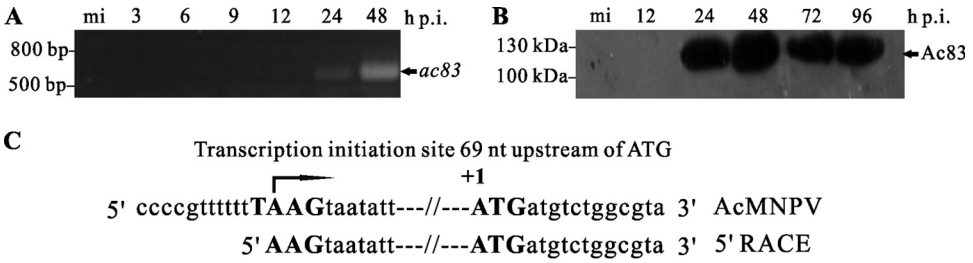

FIG 2 Transcription and expression kinetics of *ac83*. (A) RT-PCR analysis of *ac83* transcription. Total RNA was extracted from AcMNPV-infected cells at the designated time points and was used for RT-PCR analysis. A DNA marker is shown on the left. (B) Time expression profile of Ac83. Cells were either mock infected (mi) or infected with vAc83:HA at an MOI of 5 $TCID_{50}$s/cell. At different hours p.i., cells were collected and were prepared for Western blotting. Transferred proteins were detected with an anti-HA antibody. A protein marker is shown on the left. (C) Transcriptional mapping of the initiation site of *ac83* using 5′ RACE analysis. The AcMNPV genome sequence and 5′ RACE sequencing results are shown. The translation start codon of Ac83 is shown in boldface and is designated +1, and the typical baculovirus late gene promoter consensus motif TAAG is also shown in boldface. The arrow indicates the location of the transcription initiation site of *ac83*.

To further assess the effect of *ac83* deletion on virus replication, virus growth curve analysis was performed. Sf9 cells were transfected with vAc83KO, vAc83:HA, or vAcWT individually; the supernatants were collected at the time points indicated in Fig. 3C; and the BV titers were determined using a $TCID_{50}$ endpoint dilution assay. No BV titers could be detected in the vAc83KO-transfected cells at any time p.t., indicating that no infectious BVs were produced (Fig. 3C). In contrast, Sf9 cells transfected with vAc83:HA or vAcWT displayed normal and comparable increases in BV titers (Fig. 3C). These results demonstrated that deletion of *ac83* led to a defect in infectious BV production.

In order to determine whether noninfectious BVs were produced in vAc83KO-transfected Sf9 cells, Western blotting was performed to compare the levels of the major capsid protein VP39 in the supernatants of the cells transfected with each of the bacmids. As shown in Fig. 3D, VP39 was detected in the extracts of cells transfected with vAc83KO, vAc83:HA, or vAcWT, indicating that *ac83* deletion did not affect *vp39* expression. However, VP39 was detected in the supernatants of vAc83:HA- and vAcWT-transfected cells only. No band was detected in the supernatants of Sf9 cells transfected with vAc83KO (Fig. 3D), indicating that *ac83* deletion resulted in a defect in BV production.

***ac83* is not required for viral DNA replication.** To determine whether *ac83* deletion affects viral DNA replication, qPCR was performed. A *38K*-knockout AcMNPV (vAc38kKO), in which the *38K* gene was replaced with a *Cm* gene cassette, was used as a noninfectious control, because vAc38kKO is unable to spread infection from cell to cell but does not affect viral DNA replication (34). Total cellular DNA was isolated from cells transfected with vAc83KO or vAc38kKO at 12, 24, 48, and 72 h p.t. and was treated with DpnI to eliminate input bacmid DNA. The amount of viral DNA replication in the vAc83KO-transfected Sf9 cells was comparable to that in vAc38kKO-transfected cells (Fig. 4), indicating that *ac83* deletion did not affect viral DNA synthesis.

***ac83* is essential for nucleocapsid assembly.** To determine the effect of *ac83* deletion on virion morphogenesis, thin sections of vAcWT-, vAc83KO-, and vAc83:HA-transfected Sf9 cells at 60 h p.t. were observed with an electron microscope. As expected, cells transfected with vAc83:HA displayed characteristics similar to those of vAcWT-transfected cells, as demonstrated by the formation of a net-shaped virogenic stroma interspersed with rod-shaped electron-dense nucleocapsids (Fig. 5A and B) and by multiply enveloped mature nucleocapsids within the ring zone or embedded in the developing polyhedra (Fig. 5C). However, in vAc83KO-transfected cells, although a typical VS and virus-induced microvesicles could be formed (Fig. 5D and E), masses of elongated, rod-shaped electron-lucent nucleocapsid-like structures were present in the ring zone and adjacent to the inner nuclear membrane (Fig. 5F). These structures seemed to lack an electron-dense core indicative of nucleoprotein that contains viral DNA, suggesting that nucleocapsid assembly might be interrupted. A large number of circular electron-dense bodies appeared near the VS stromal matte (Fig. 5G); these are often observed in cells with abnormal nucleocapsids (44). In addition, although most vAc83KO-transfected cells contained elongated electron-lucent structures that were apart from the virogenic stroma and localized to the inner nuclear membrane, these aberrant structures could occasionally be observed at the electron-dense edges of the virogenic stroma in a few vAc83KO-transfected cells (Fig. 5H). No virions were embedded in the polyhedra in the vAc83KO-transfected cells (Fig. 5I). Taken together, these observations indicated that deletion of *ac83* affected nucleocapsid assembly.

Expression of Ac83 aa 451 to 600 is sufficient to rescue infectious BV production. AcMNPV *ac83* encodes a polypeptide of 847 aa residues with a predicted molecular mass of approximately 96 kDa. To define the functional domains of Ac83 required for infectious BV production, a gene truncation strategy generating N- and C-terminal deletion variants of Ac83 was implemented. A set of fragments encoding both N- and C-terminally truncated variants of Ac83 was produced by using the overlap PCR technique, cloned into the donor plasmid pFB1-PH-GFP, and then inserted into bAc83KO. The abilities of the *ac83*-truncated variants to rescue infectious BV production were monitored by fluorescence microscopy and were determined by a $TCID_{50}$ endpoint dilution assay. As shown in Fig. 6A and B, although protein database mining demonstrated that Ac83 contains a putative INM-SM, a CBD, and a PR region (Fig. 1), none of these play a role in infectious BV production, as evidenced by the fact that similar growth kinetics were found for vAc83:delSM, vAc83:delCBD, vAc83:delPR, and vAc83:HA. In addition, the deletion of the N-terminal 290 aa residues of Ac83 (vAc83:del2-290) had no effect on infectious BV production, as evidenced by similar growth kinetics for vAc83:del2-290 and vAc83:HA. Further truncation of Ac83 up to the N-terminal 450 aa residues (vAc83:del2-450) still resulted in almost complete rescue of infectious BV production.

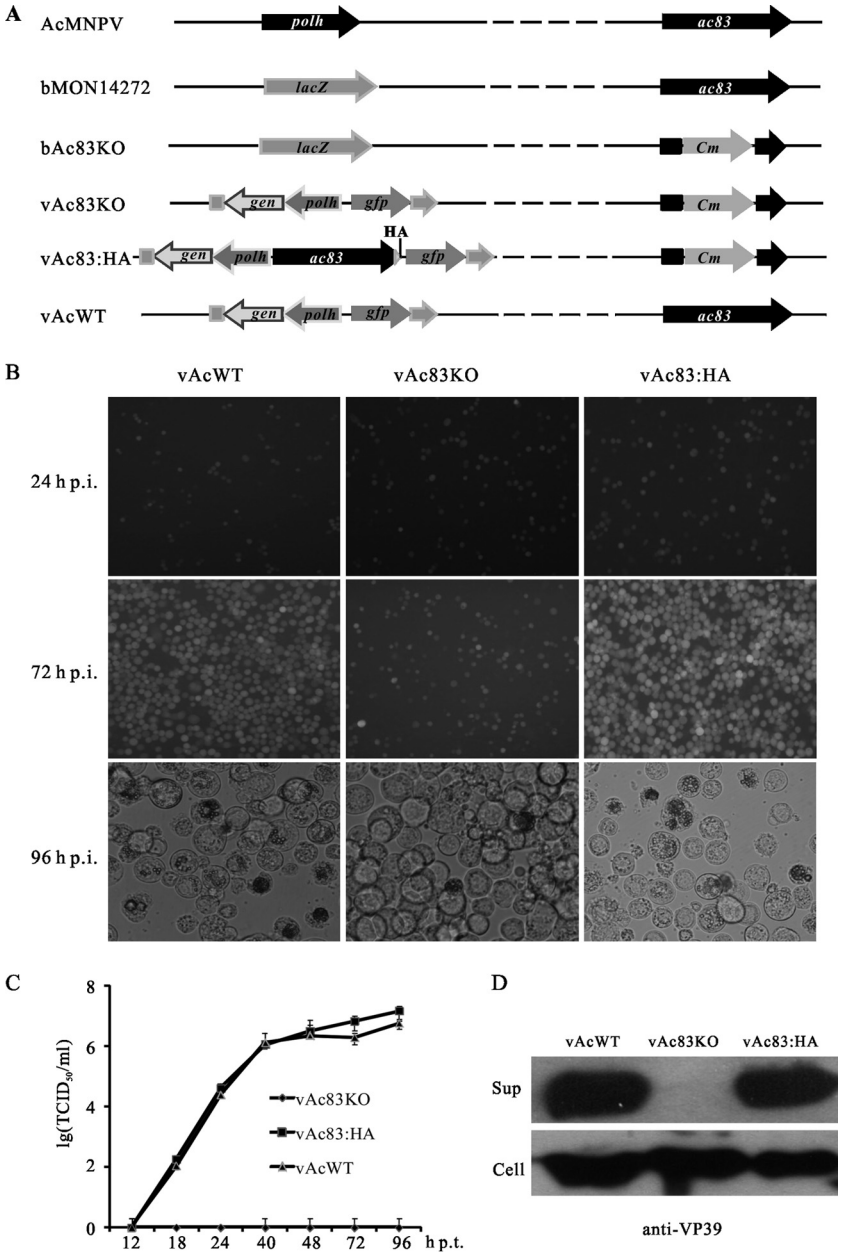

FIG 3 Construction of recombinant viruses and analysis of viral replication. (A) Schematic diagram of the recombinant viruses used in this study. The bacmid bAc83KO was constructed by replacing a 2,057-bp fragment of *ac83* in the bMON14272 genome with a 1,038-bp *Cm* cassette via ET homologous recombination in *Escherichia coli*. The *ac83* deletion virus (vAc83KO) was constructed by inserting the *polh* and *gfp* genes into the *polh* locus of bAc83KO by Tn*7*-mediated transposition. The *ac83* rescue virus (vAc83:HA) was constructed by transposing the *ac83* ORF tagged with an HA epitope (triangle) under the control of its native promoter together with the *polh* and *gfp* genes into the *polh* locus of bAc83KO. The wild-type control virus (vAcWT) was constructed by transposing the *polh* and *gfp* genes into the *polh* locus of bMON14272. (B) Sf9 cells were transfected with vAcWT, vAc83KO, or vAc83:HA. At the indicated time points p.t., cells were monitored for infection by a fluorescence microscope. (C) The production of infectious BVs in the supernatants of transfected cells was determined by $TCID_{50}$ endpoint dilution assays. Each data point was determined from the average for three independent transfections. Error bars represent standard deviations. (D) The supernatants (Sup) and cell extracts (Cell) of transfected cells at 96 h p.t. were separated by SDS-PAGE and were analyzed by Western blotting with anti-VP39 to detect the major capsid protein VP39.

At 96 h p.i., the BV titer of vAc83:del2-450 was only 4-fold lower than that of vAc83:HA. C-terminal truncation of Ac83 revealed that the deletion of Ac83 aa 742 to 847 (vAc83:del742-847) had no significant effect on infectious BV production. After the removal of Ac83 aa 601 to 847 (vAc83:del601-847), the virus propagated, although the ability to produce progeny virus was attenuated to some extent: the titer at 96 h p.i. was approximately 100-fold lower than that of vAc83:HA. An Ac83 construct with a further truncation, of Ac83 aa 551 to 847 (vAc83:del551-847), completely failed to rescue infectious BV production. Finally, unexpectedly, a construct from which both the N-terminal amino acid residues 2 to 450 and the C-terminal amino acid residues 601 to 847 of Ac83

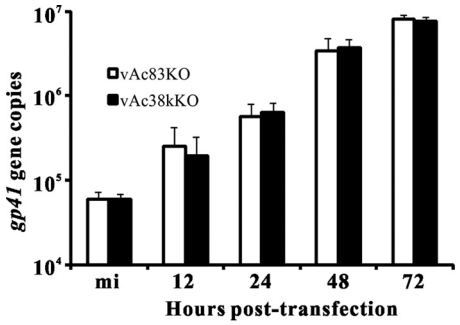

FIG 4 Real-time PCR analysis of viral DNA synthesis. Sf9 cells were transfected in triplicate with vAc83KO or vAc38kKO. At the designated time points p.t., total intracellular DNA was isolated, digested with the restriction enzyme DpnI to eliminate input bacmid DNA, and analyzed by real-time PCR. The results are averages for three independent replication assays. Error bars indicate standard deviations.

were removed (vAc83:del2-450/601-847) still showed virus propagation, although the ability of this truncation form of Ac83 to rescue virus production was severely compromised. The expression of truncated Ac83 was examined by Western blotting and exhibited a level comparable to that of full-length Ac83 (data not shown). In the viruses with C-terminal truncations (vAc83:del742-847, vAc83:del601-847, vAc83:del551-847, and vAc83:del2-450/601-847), there are no overlaps between the repaired fragments and the remaining 3′-terminal sequences of *ac83* in the deletion locus, so intragenomic recombination would be impossible. Furthermore, no intragenomic recombination was detected in other Ac83 truncation variants (vAc83:delSM, vAc83:delCBD, vAc83:delPR, vAc83:del2-290, and vAc83:del2-450) by PCR analysis (data not shown). Taken together, these results demonstrate that the most important region of Ac83 for infectious BV production is located between Ac83 aa 451 and 600.

The CBD of Ac83 is essential for the efficient establishment of *per os* infection. Ac83 contains a typical type II CBD that possibly interacts with the chitin component of insects and has been postulated to play a role in baculovirus primary infection (17). A recent study found that Ac83 was a component of the PIF complex on the ODV envelope, which further suggested that Ac83 might play a role in baculovirus *per os* infection (19). To determine the *in vivo* effect of deletion of the Ac83 CBD, BVs and OBs of vAc83:delCBD, vAc83:HA, and vAcWT from transfected Sf9 cells were bioassayed in 4th-instar *T. ni* larvae. Intrahemocoelic injection of

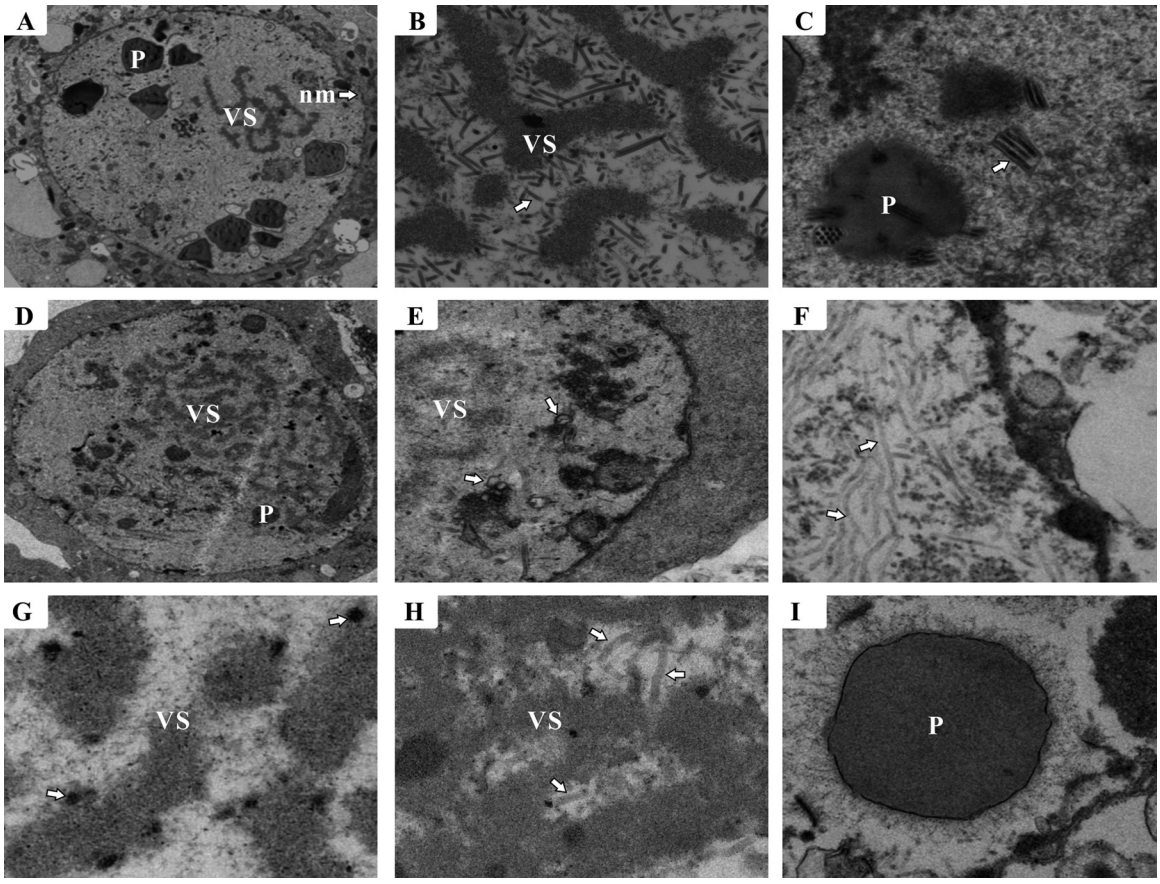

FIG 5 Electron microscopy of Sf9 cells transfected with vAc83KO or vAc83:HA. (A to C) Cells transfected with vAc83:HA. (A) Portion of a cell showing the virogenic stroma (VS), polyhedra (P), and nuclear membrane (nm) (arrow). (B) Rod-shaped nucleocapsids (arrow) within the electron-dense edges of the VS. (C) Multiply enveloped mature ODVs (arrow) and polyhedra with ODVs embedded. (D to I) Cells transfected with vAc83KO. (D) VS. (E) Portion of the cell region showing microvesicles (arrows) in the nucleus. (F) Cluster of elongated, electron-lucent tubular structures that localized near the inner nuclear membrane (arrows). (G) VS devoid of nucleocapsids and exhibiting electron-dense bodies (arrows). (H) Nucleus with aberrant tubular structures (arrows) within the VS. (I) Polyhedra devoid of embedded virions.

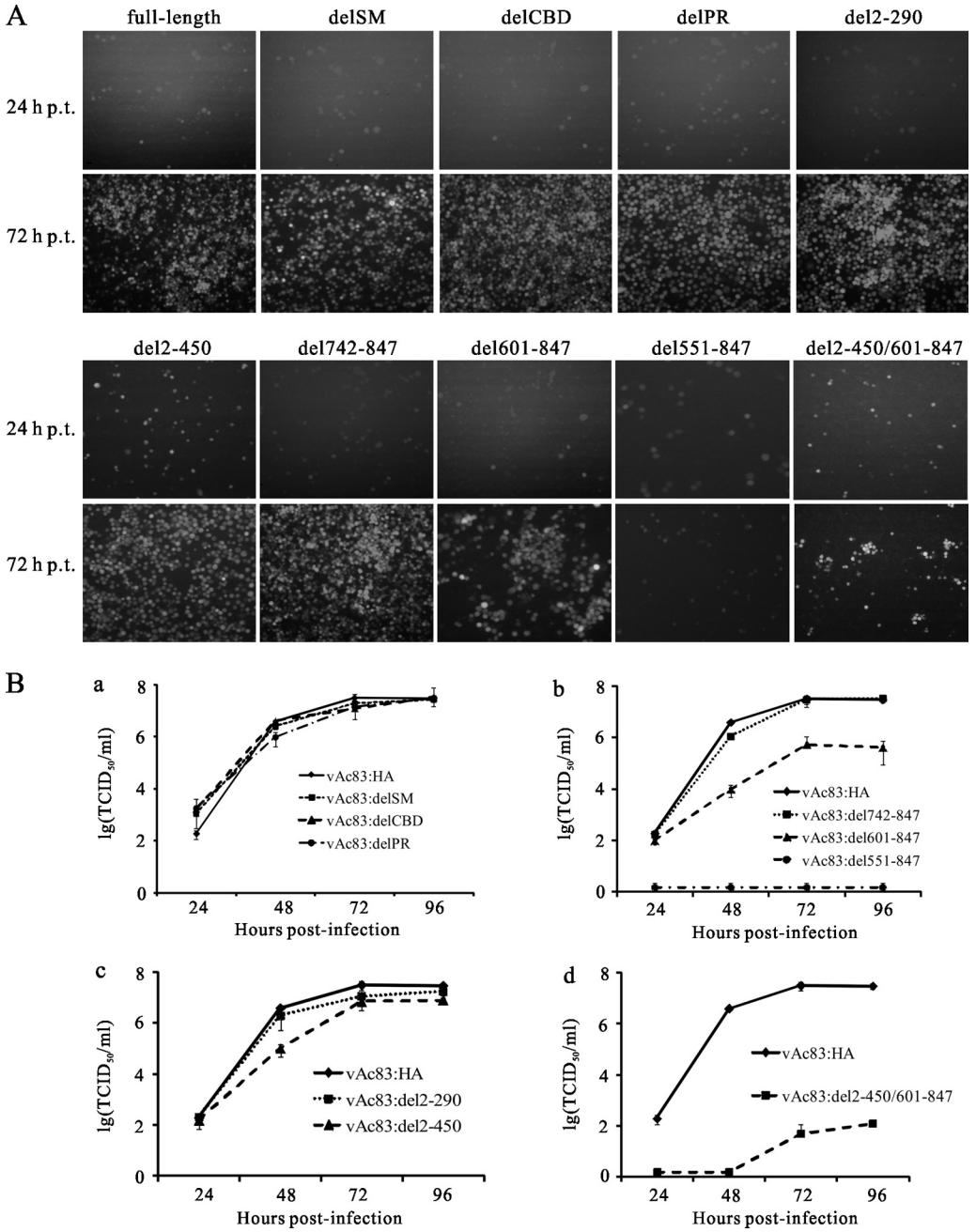

FIG 6 Expression of Ac83 aa 451 to 600 is sufficient to rescue infectious BV production. (A) Abilities of different Ac83 truncation viruses to rescue infectious BV production. Sf9 cells were transfected with the indicated bacmid, and virus propagation was monitored by fluorescence microscopy at the indicated time points p.t. (B) One-step growth curves of the bAc83KO genome repaired with a virus from which the INM-SM, the CBD, or the PR region of Ac83 was deleted (a) or with a virus in which Ac83 was N-terminally truncated (b), C-terminally truncated (c), or both N- and C-terminally truncated (d). Sf9 cells were infected with the indicated viruses at an MOI of 0.1 $TCID_{50}$/cell, and at the designated time points p.i., the supernatants were harvested and were analyzed for the release of infectious BVs by a $TCID_{50}$ endpoint dilution assay. Data points are averages of titers derived from three independent infections. Error bars represent standard deviations.

the vAc83:delCBD BV supernatant into larvae at 5 $TCID_{50}$s/larva resulted in a mortality rate similar to that with vAc83:HA or vAcWT (Table 2). Similar results were obtained at doses of 10 or 50 $TCID_{50}$s/larva (data not shown), suggesting that deletion of the Ac83 CBD did not affect BV infectivity. However, bioassays with OBs revealed significant differences in oral infectivity between the three viruses. OBs of vAc83:HA and vAcWT produced similar mortality rates, and no significant difference in the median lethal dose (LD_{50}) was observed (Table 2). In contrast, feeding the larvae with as many as 1×10^4 OBs of vAc83:delCBD caused almost no mortality, and only 58.3% mortality was achieved when the larvae were administered a high dose of 5×10^6 OBs/larva (Table 2), suggesting that deletion of the Ac83 CBD severely attenuated the oral infectivity of AcMNPV.

TABLE 2 Infectivities of vAcWT, vAc83:HA, and vAc83:delCBD in 4th-instar *T. ni* larvae[a] and the effect of calcofluor white on the infectivity of vAc83:delCBD

Inoculation method and virus or control	Dosage	Mortality (%) by 6 days p.i.	LD_{50}[b] (95% confidence interval)
Injection			
vAcWT	5 $TCID_{50}$s	100	
vAc83:HA	5 $TCID_{50}$s	100	
vAc83:delCBD	5 $TCID_{50}$s	100	
H_2O		4.1[c]	
Per os			
vAc83:delCBD	1×10^4 OBs	8.3	
	5×10^6 OBs	58.6	
H_2O		0	
vAcWT			123.2 (92.5–164.1) A
vAc83:HA			144.9 (108.3–194.1) A
vAc83:delCBD + calcofluor white			1.5×10^5 (7.9×10^4-2.7×10^5) B

[a] A total of 24 larvae were used for each treatment.
[b] Expressed as OBs/larva. Values followed by different capital letters are significantly different from each other.
[c] Larval death not due to virus infection (microscopy and PCR analysis).

Since deletion of the Ac83 CBD severely compromised oral infectivity, it is possible that any changes in OB morphogenesis upon the deletion of the Ac83 CBD might account for the defect. Thus, OB formation was observed using electron microscopy. Mature OBs containing ODVs were observed in both vAc83:delCBD- and vAc83:HA-infected Sf9 cells and were morphologically indistinguishable (Fig. 7).

Previous studies have shown that disruption of the PM enhances larval susceptibility to baculovirus infection (39), and some baculoviruses encode a kind of protease called enhancin, which disrupts the PM (45). Moreover, the chemical reagent calcofluor white is able to bind chitin so as to disrupt the PM, thus enhancing baculovirus infectivity (39). Considering the presence of the CBD, Ac83 may play a role in the disruption of the PM to facilitate the passage of ODVs. If so, disruption of the PM should enhance the oral infectivity of vAc83:delCBD. Therefore, bioassays of vAc83:delCBD in the presence of calcofluor white were performed. Larvae treated with calcofluor white displayed higher susceptibility than untreated larvae (data not shown). The LD_{50} of vAc83:delCBD in calcofluor white-treated 4th-instar *T. ni* larvae was 1.5×10^5 OBs/larva. However, the calcofluor white treatment did not completely rescue the oral infectivity of vAc83:delCBD; the LD_{50} of vAc83:delCBD in insects treated with calcofluor white was still approximately 3 log units higher than that of vAcWT

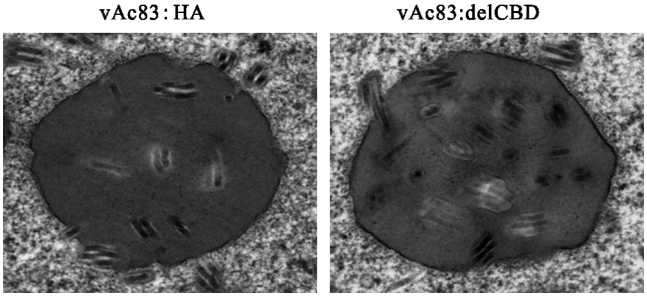

FIG 7 Electron microscopy of Sf9 cells infected with vAc83:HA or vAc83:delCBD. Sf9 cells were infected with vAc83:HA or vAc83:delCBD at an MOI of 5 $TCID_{50}$s/cell. At 60 h p.t., cells were prepared for electron microscopy analysis.

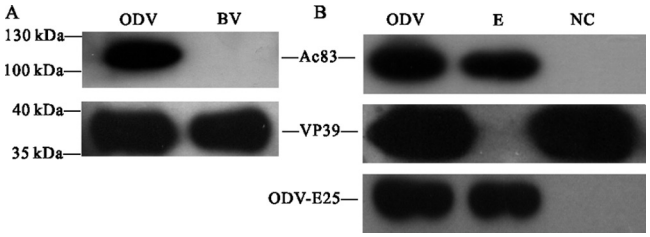

FIG 8 Localization of Ac83 in purified and fractionated virions. BVs and ODVs were purified from vAc83:HA-infected Sf9 cells, and the purified ODVs were further fractionated into envelope (E) and nucleocapsid (NC) fractions. Protein samples were subjected to Western blotting in order to determine the localization profile of Ac83 in purified BVs and ODVs (A) or fractionated ODVs (B). Proteins were detected by immunoblotting with an anti-HA antibody to detect HA-tagged Ac83, with anti-ODV-E25 to detect the BV/ODV envelope-associated protein ODV-E25, and with an anti-VP39 antibody to detect the major capsid protein VP39.

(123.2 OBs/larva) or vAc83:HA (144.9 OBs/larva) (Table 2). Therefore, the bioassay results suggested that the Ac83 CBD might have other targets in addition to the PM, such as microvilli.

Ac83 localizes specifically to the ODV envelope. Previous results concerning the localization profile of Ac83 and its homologs in virions were ambiguous. Although OpP91 has been demonstrated to be a component of both the BVs and the ODVs of *Orgyia pseudotsugata* NPV and localized predominantly to capsids, proteomic analyses of the BVs and ODVs of AcMNPV and *Helicoverpa armigera* NPV suggested that Ac83 and VP91 (the *Helicoverpa armigera* NPV homolog) belonged to the ODV envelope-specific component (23, 25, 46). In the present study, BVs and ODVs purified from vAc83:HA-infected Sf9 cells were analyzed by Western blotting to determine the localization of Ac83. As shown in Fig. 8A, Ac83 is specifically localized to the purified AcMNPV ODVs but not to BVs. The purified ODVs were further fractionated into envelope and nucleocapsid fractions, and Ac83 was detected in the ODV envelope fraction. The major capsid protein VP39 and the BV/ODV envelope-associated protein ODV-E25, used as controls, could be detected only in the expected fractions (Fig. 8B). Thus, these results demonstrated that Ac83 is an ODV envelope-specific protein, a finding consistent with previous proteomic results (23, 24).

Ac83 contains a functional INM-SM. It has been shown previously that the N-terminal 23 aa of ODV-E66, one of the ODV envelope proteins of AcMNPV, are sufficient to traffic fusion proteins to intranuclear membranes and the ODV envelope, and this sequence has been termed an INM-SM (47, 48). A typical INM-SM contains two features: (i) a hydrophobic domain of approximately 18 aa and (ii) a positively charged amino acid within aa 4 to 8 from the end of the hydrophobic domain that is positioned on the cytoplasmic or nucleoplasmic side of the membrane (48). The INM-SM is found not only in several ODV proteins but also in many inner nuclear envelope proteins of eukaryotes (47, 49). Ac83 has been predicted to have an INM-SM similar to that of ODV-E66 (Fig. 9A) (50). To investigate whether the INM-SM of Ac83 is functional, Ac83 INM-SM-GFP fusion proteins were monitored to determine their localization in relation to the absence or presence of viral infection. Sf9 cells either were transfected with pIB-SM-GFP or were infected with vAcSM-GFP at an MOI of 5 $TCID_{50}$s/cell. When the GFP fusion protein was transiently expressed in Sf9 cells, it localized almost exclusively in the

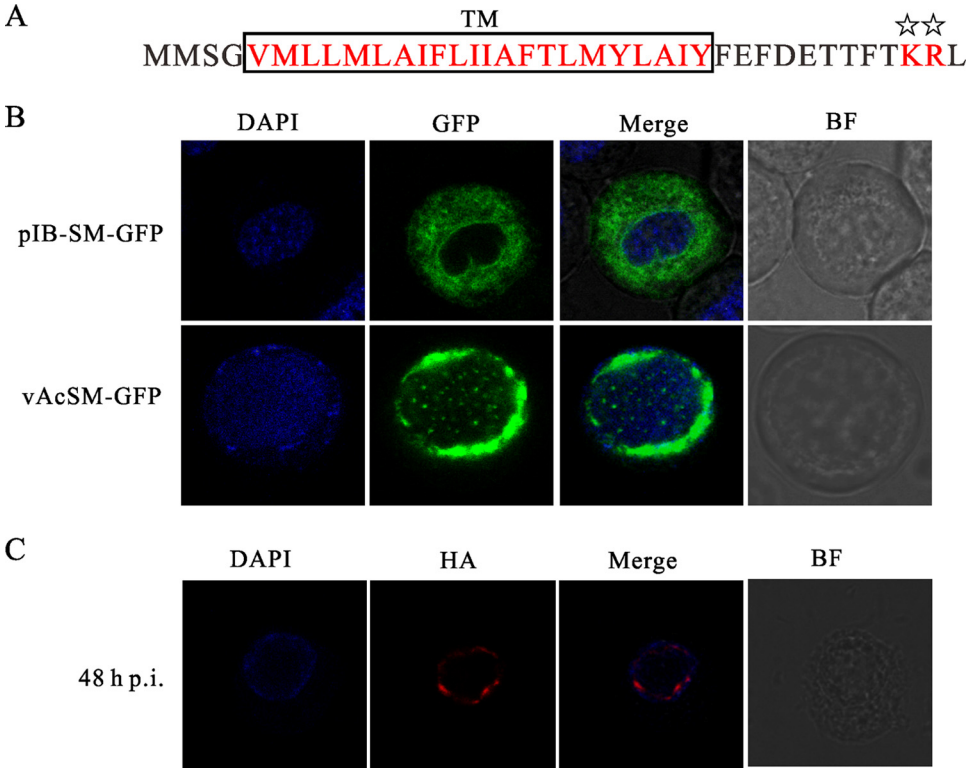

FIG 9 Ac83 contains a functional inner nuclear membrane sorting motif and is localized to the nuclear periphery during infection. (A) Schematic representation of two characteristics of the INM-SM of Ac83. The highly hydrophobic TM is boxed and shown in red. The conserved positively charged amino acids are also shown in red and are marked with stars. (B and C) Confocal microscopy. (B) Sf9 cells were transfected with pIB-SM-GFP (top) or were infected with vAcSM-GFP (bottom) at an MOI of 5 $TCID_{50}$s/cell. At 24 h p.t. or 48 h p.i., the cells were prepared for monitoring of the localization profile of GFP (green). (C) Sf9 cells were infected with vAc83:HA at an MOI of 5 $TCID_{50}$s/cell. At 48 h p.i., the cells were fixed, probed with a mouse monoclonal anti-HA antibody to detect HA-tagged Ac83, and visualized using Alexa Fluor 647-conjugated goat anti-mouse IgG (red). The cells were stained with DAPI to directly visualize nuclear DNA (blue). BF, bright-field microscopy.

cytoplasm and formed a rim around the nucleus (Fig. 9B). In the context of infection, GFP fluorescence accumulated at the periphery of the nucleus and formed large foci near the INM (Fig. 9B). The localization pattern of the chimeric INM-SM-GFP was very similar to that of the well-characterized INM-SM of ODV-E66 (47, 49).

The subcellular localization pattern of Ac83 was also examined in vAc83:HA-infected Sf9 cells. The HA-tagged Ac83 was probed with a mouse monoclonal antibody against HA, visualized by Alexa Fluor 647-conjugated goat anti-mouse IgG, and examined using laser scanning confocal microscopy. Discrete foci with red fluorescence appeared near the INM at 24 h p.i. and became concentrated at 48 h p.i. (Fig. 9C). By 72 h p.i., the concentration of fluorescence in the nucleus was more pronounced, as larger foci formed around the periphery of the nucleus (data not shown). Taken together, the results described above suggested that Ac83 contains a functional INM-SM that guides it to anchor the INM and the ODV envelope.

DISCUSSION

ac83 is one of the 37 baculovirus core genes, but its role in the AcMNPV life cycle is unknown. Here we demonstrate that *ac83* plays multiple roles in the baculovirus life cycle. *ac83* is essential for AcMNPV nucleocapsid assembly and for efficient establishment of *per os* infection, thus providing a rationale for its essential role as a core gene.

To investigate the functional role of *ac83* in the baculovirus life cycle, we generated an *ac83*-knockout virus and observed that *ac83* was essential for nucleocapsid assembly (Fig. 5). In vAc83KO-transfected Sf9 cells, a mass of abnormal electron-lucent tubular structures was observed in the ring zone or adjacent to the inner nuclear membrane; however, deletion of *ac83* did not affect viral DNA replication (Fig. 5). The results were entirely consistent with the most recent study on *BmP95* (20).

Truncation analysis revealed that expression of Ac83 aa 451 to 600, which constitute approximately one-fifth of full-length (847-aa) Ac83, resulted in the formation of infectious BVs, although production was severely compromised (Fig. 6). It has been observed that repair of the N-terminal 500 aa of BmP95 could not rescue the function of BmP95 (20). Similarly, in our study, repair of the N-terminal 550 aa of Ac83, corresponding to the truncation of Ac83 aa 551 to 847 (vAc83:del551-847), completely failed to rescue infectious BV production (Fig. 6). These results indicated that the functional domains required for infectious BV production reside in Ac83 aa 451 to 600; while the other parts of Ac83 are not strictly essential, their presence contributes significantly to the fitness of the virus.

Examination of Ac83 aa 451 to 600 revealed a potential nuclear localization signal (NLS), ^{597}KRPK^{600} (data not shown), which may function in the nuclear transport of Ac83. However, repair of Ac83 aa 451 to 596 (disruption of both the INM-SM and the

predicted NLS) still resulted in infectious BV production (data not shown), implying that there are unidentified signals targeting this fragment of Ac83 to the nucleus.

Baculoviruses initiate infection through an oral infection route when the insects consume food contaminated with OBs. ODVs are released from OBs under the alkaline conditions of the midguts of larvae and carry with them a battery of proteins, named PIFs, to infect the midgut epithelia of host larvae. Before the infection of epithelia, ODVs encounter a barrier: the PM. A few lepidopteran NPVs and GVs encode a class of metalloproteinases called enhancins, which degrade the mucin component of the PM (45). However, it is not clear how baculoviruses without enhancins pass through the PM. For example, though highly infectious, AcMNPV does not encode an enhancin (17). The PM is not the functional target of identified PIFs (51). However, the PMs of *T. ni* larvae were degraded upon inoculation of either wild-type AcMNPV or AcMNPV with *p74* deleted (10). Thus, there must be unidentified proteins in AcMNPV that play pivotal roles in the disruption of the PM or the passage of ODVs through the PM. In this study, we observed that deletion of the Ac83 CBD resulted in the failure of *per os* infection of *T. ni* with AcMNPV.

Chitin is generally essential for the function of chitin/protein structures (52). Interference with the chitin component of the PM often leads to a defect in the integrity and normal function of the PM (53, 54). Calcofluor white, a chemical reagent with chitin-binding properties, blocks PM formation, disassociates the PM by acting as a chitin-binding competitor, and concomitantly causes the loss of protection of the insect from baculovirus infection (39). Thus, targeting of the chitin component by using a chitin-binding reagent promises to be an ideal strategy for blocking PM protein formation (55). AcMNPV encodes four proteins with the potential to bind chitin: Ac83, Ac145, Ac150, and Ac64 (GP37) (17). Although Ac145 and Ac150 contain CBDs, these proteins have not been detected in the PIF complex (19). Ac64 (GP37), which resembles the entomopoxvirus protein spheroidin, has been shown to be associated with polyhedra but not with ODVs and is not essential for baculovirus replication *in vivo* or *in vitro* (56, 57). Ac83 contains a type II CBD and may possess the ability to bind chitin. Unfortunately, we did not observe any chitin-binding ability of Ac83 *in vitro* (data not shown). Nevertheless, because deletion of the Ac83 CBD resulted in the failure of *per os* AcMNPV infection and because Ac83 is a component of the PIF complex on the ODV envelope, we logically speculate that the affinity of Ac83 for chitin could possibly disrupt the spatial structure and, concomitantly, the integrity of the PM, thus facilitating the passage of ODVs. In accordance with this hypothesis, bioassays indicated that disruption of the PM with calcofluor white could partially rescue the oral infectivity of vAc83:delCBD, suggesting that the PM is a functional target of Ac83 (Table 2).

GVs have a set of 23 specific genes that are not present in NPVs (58), and one remarkable characteristic of GVs is the universal presence of metalloproteinase homologs in their genomes (17). One of these metalloproteinases is a stromelysin-1-like metalloproteinase encoded by a GV-specific gene (17). Stromelysin-1 is an enzyme that is involved in the breakdown of the extracellular matrix and in tissue remodeling (59, 60). Thus, the metalloproteinase homologs in GVs may facilitate the passage of GVs through the PM and may explain why the Ac83 CBD is conserved in NPVs but is poorly conserved in GVs (Fig. 1).

It is currently unclear whether ODVs diffuse randomly to access the midgut epithelium. Previous studies have demonstrated that infected midgut cells are unstable and frequently are sloughed into the gut lumen, an effective strategy used by lepidopteran hosts to defend against virus infection (61). In addition, midgut cells are also prone to apoptosis during development (62). Therefore, ODVs must establish infection efficiently and effectively, because the infection of target cells is a race against time. Not only is chitin a component of the PM; it is also associated with midgut epithelial cells. The chitin component of the PM is produced by chitin synthase, a plasma membrane-embedded enzyme located at the apical tips of brush border microvilli (17). Therefore, an affinity of Ac83 for the chitin of the midgut epithelial cells may offer evolutionary advantages by facilitating the passage of ODVs through the PM or the interaction of ODVs with the insect epithelial cells, possibilities consistent with our bioassay results. Another ODV envelope protein, ODV-E66, may also have a function similar to that of Ac83. ODV-E66 has been shown to play an important role in oral infection with AcMNPV (63). ODV-E66 encodes a novel chondroitinase that efficiently digests chondroitin and has been postulated to play a role in viral infection of the epithelial cells or in the disintegration of the infected host (64). Therefore, from an evolutionary viewpoint, we do not suppose random diffusion is utilized by baculovirus ODVs in the process of infecting midgut epithelial cells, because it is not an efficient mechanism for the rapid establishment of a primary infection. In view of the roles of Ac83 and ODV-E66 in the *per os* infection process of AcMNPV, we hypothesize that Ac83 and ODV-E66 may represent a class of proteins that facilitate the efficient establishment of infection with ODVs in the insect midgut.

Perusal of the N-terminal sequences of Ac83 homologs revealed a C2HC-type zinc finger that was conserved in all Ac83 homologs (Fig. 1). The C2HC-type zinc finger was first identified in myelin transcription factor I, a transcription factor that binds to the *cis*-regulatory elements and thus regulates the expression of a gene specific to glia, the myelin proteolipid protein gene (65). Subsequently, it was found that the C2HC-type zinc finger could be directly involved in protein-protein interactions (41). Interestingly, protein mining using Uniprot or ExPASy identified two type II CBDs in Ac83, the first of which overlaps with the predicted zinc finger of Ac83 (data not shown). Analysis indicated that the first type II CBD identified is incomplete compared with the second one (data not shown). Considering that the zinc finger motif and type II CBDs are both rich in cysteine, we hypothesized that the first type II CBD is a putative zinc finger motif. Most importantly, sequence analysis of other components of the PIF complex revealed that nearly all of them potentially contain one or more types of zinc finger (data not shown). In addition, Ac83 also contains a PR region that, while it plays no role in infectious BV production (Fig. 6), may function in protein-protein interactions, such as the interaction of Ac83 with other PIF components. Considering that the PIF complex components are possibly arranged in a noncovalent manner (66), it is intriguing to hypothesize that the putative C2HC zinc finger motif, together with the PR region, may play a pivotal role in the association of Ac83 with other PIF complex components.

In summary, it is intriguing to speculate that Ac83 may represent another type of PIF that not only participates in *per os* infection but may also perform other pivotal roles in the baculovirus life cycle. To the best of our knowledge, Ac83 is the first baculovi-

rus protein that functions both in nucleocapsid assembly and in *per os* infectivity.

ACKNOWLEDGMENTS

This research was supported by the National Basic Research Program of China (973 Program; grant 2009CB118903), the National Nature Science Foundation of China (grant 30900941), the Hi-Tech Research and Development Program of China (863 Program; grant 2011AA10A204), and the Fundamental Research Funds for the Central Universities (grant 09lgpy39).

REFERENCES

1. **Herniou EA, Olszewski JA, Cory JS, O'Reilly DR.** 2003. The genome sequence and evolution of baculoviruses. Annu. Rev. Entomol. **48:**211–234.
2. **Jehle JA, Blissard GW, Bonning BC, Cory JS, Herniou EA, Rohrmann GF, Theilmann DA, Thiem SM, Vlak JM.** 2006. On the classification and nomenclature of baculoviruses: a proposal for revision. Arch. Virol. **151:**1257–1266.
3. **Zanotto PM, Kessing BD, Maruniak JE.** 1993. Phylogenetic interrelationships among baculoviruses: evolutionary rates and host associations. J. Invertebr. Pathol. **62:**147–164.
4. **Lung O, Westenberg M, Vlak JM, Zuidema D, Blissard GW.** 2002. Pseudotyping *Autographa californica* multicapsid nucleopolyhedrovirus (AcMNPV): F proteins from group II NPVs are functionally analogous to AcMNPV GP64. J. Virol. **76:**5729–5736.
5. **Ayres MD, Howard SC, Kuzio J, Lopez-Ferber M, Possee RD.** 1994. The complete DNA sequence of *Autographa californica* nuclear polyhedrosis virus. Virology **202:**586–605.
6. **Yuan M, Huang Z, Wei D, Hu Z, Yang K, Pang Y.** 2011. Identification of *Autographa californica* nucleopolyhedrovirus *ac93* as a core gene and its requirement for intranuclear microvesicle formation and nuclear egress of nucleocapsids. J. Virol. **85:**11664–11674.
7. **Garavaglia MJ, Miele SA, Iserte JA, Belaich MN, Ghiringhelli PD.** 2012. The *ac53*, *ac78*, *ac101*, and *ac103* genes are newly discovered core genes in the family *Baculoviridae*. J. Virol. **86:**12069–12079.
8. **Braunagel SC, Summers MD.** 1994. *Autographa californica* nuclear polyhedrosis virus, PDV, and ECV viral envelopes and nucleocapsids: structural proteins, antigens, lipid and fatty acid profiles. Virology **202:**315–328.
9. **Slack J, Arif BM.** 2007. The baculoviruses occlusion-derived virus: virion structure and function. Adv. Virus Res. **69:**99–165.
10. **Faulkner P, Kuzio J, Williams GV, Wilson JA.** 1997. Analysis of p74, a PDV envelope protein of *Autographa californica* nucleopolyhedrovirus required for occlusion body infectivity *in vivo*. J. Gen. Virol. **78**(Part 12)**:**3091–3100.
11. **Kikhno I, Gutierrez S, Croizier L, Croizier G, Ferber ML.** 2002. Characterization of *pif*, a gene required for the *per os* infectivity of *Spodoptera littoralis* nucleopolyhedrovirus. J. Gen. Virol. **83:**3013–3022.
12. **Pijlman GP, Pruijssers AJ, Vlak JM.** 2003. Identification of *pif-2*, a third conserved baculovirus gene required for *per os* infection of insects. J. Gen. Virol. **84:**2041–2049.
13. **Fang M, Nie Y, Harris S, Erlandson MA, Theilmann DA.** 2009. *Autographa californica* multiple nucleopolyhedrovirus core gene *ac96* encodes a per os infectivity factor (*pif-4*). J. Virol. **83:**12569–12578.
14. **Ohkawa T, Washburn JO, Sitapara R, Sid E, Volkman LE.** 2005. Specific binding of *Autographa californica* M nucleopolyhedrovirus occlusion-derived virus to midgut cells of *Heliothis virescens* larvae is mediated by products of *pif* genes *Ac119* and *Ac022* but not by *Ac115*. J. Virol. **79:**15258–15264.
15. **Harrison RL, Sparks WO, Bonning BC.** 2010. *Autographa californica* multiple nucleopolyhedrovirus ODV-E56 envelope protein is required for oral infectivity and can be substituted functionally by *Rachiplusia ou* multiple nucleopolyhedrovirus ODV-E56. J. Gen. Virol. **91:**1173–1182.
16. **Nie Y, Fang M, Erlandson MA, Theilmann DA.** 2012. Analysis of the *Autographa californica* multiple nucleopolyhedrovirus overlapping gene pair *lef3* and *ac68* reveals that AC68 is a *per os* infectivity factor and that LEF3 is critical, but not essential, for virus replication. J. Virol. **86:**3985–3994.
17. **Rohrmann GF.** 2011. Baculovirus molecular biology. U.S. National Library of Medicine, National Center for Biotechnology Information, Bethesda, MD.
18. **Simon O, Palma L, Williams T, Lopez-Ferber M, Caballero P.** 2012. Analysis of a naturally-occurring deletion mutant of *Spodoptera frugiperda* multiple nucleopolyhedrovirus reveals *sf58* as a new *per os* infectivity factor of lepidopteran-infecting baculoviruses. J. Invertebr. Pathol. **109:**117–126.
19. **Peng K, van Lent JW, Boeren S, Fang M, Theilmann DA, Erlandson MA, Vlak JM, van Oers MM.** 2012. Characterization of novel components of the baculovirus *per os* infectivity factor complex. J. Virol. **86:**4981–4988.
20. **Xiang X, Shen Y, Yang R, Chen L, Hu X, Wu X.** 27 March 2013. *Bombyx mori* nucleopolyhedrovirus *BmP95* plays an essential role in budded virus production and nucleocapsid assembly. J. Gen. Virol. doi:10.1099/vir.0.050583-0.
21. **Tellam RL, Wijffels G, Willadsen P.** 1999. Peritrophic matrix proteins. Insect Biochem. Mol. Biol. **29:**87–101.
22. **Aguinaldo AM, Turbeville JM, Linford LS, Rivera MC, Garey JR, Raff RA, Lake JA.** 1997. Evidence for a clade of nematodes, arthropods and other moulting animals. Nature **387:**489–493.
23. **Braunagel SC, Russell WK, Rosas-Acosta G, Russell DH, Summers MD.** 2003. Determination of the protein composition of the occlusion-derived virus of *Autographa californica* nucleopolyhedrovirus. Proc. Natl. Acad. Sci. U. S. A. **100:**9797–9802.
24. **Wang R, Deng F, Hou D, Zhao Y, Guo L, Wang H, Hu Z.** 2010. Proteomics of the *Autographa californica* nucleopolyhedrovirus budded virions. J. Virol. **84:**7233–7242.
25. **Russell RL, Rohrmann GF.** 1997. Characterization of P91, a protein associated with virions of an *Orgyia pseudotsugata* baculovirus. Virology **233:**210–223.
26. **Ono C, Kamagata T, Taka H, Sahara K, Asano S, Bando H.** 2012. Phenotypic grouping of 141 BmNPVs lacking viral gene sequences. Virus Res. **165:**197–206.
27. **Marchler-Bauer A, Anderson JB, Cherukuri PF, DeWeese-Scott C, Geer LY, Gwadz M, He S, Hurwitz DI, Jackson JD, Ke Z, Lanczycki CJ, Liebert CA, Liu C, Lu F, Marchler GH, Mullokandov M, Shoemaker BA, Simonyan V, Song JS, Thiessen PA, Yamashita RA, Yin JJ, Zhang D, Bryant SH.** 2005. CDD: a Conserved Domain Database for protein classification. Nucleic Acids Res. **33:**D192–D196.
28. **Letunic I, Doerks T, Bork P.** 2009. SMART 6: recent updates and new developments. Nucleic Acids Res. **37:**D229–D232.
29. **Soding J.** 2005. Protein homology detection by HMM-HMM comparison. Bioinformatics **21:**951–960.
30. **Larkin MA, Blackshields G, Brown NP, Chenna R, McGettigan PA, McWilliam H, Valentin F, Wallace IM, Wilm A, Lopez R, Thompson JD, Gibson TJ, Higgins DG.** 2007. Clustal W and Clustal X version 2.0. Bioinformatics **23:**2947–2948.
31. **Nicholas KB, Nicholas HB, Deerfield DW.** 1997. GeneDoc: analysis and visualization of genetic variation. EMBNEW News **4:**14.
32. **Luckow VA, Lee SC, Barry GF, Olins PO.** 1993. Efficient generation of infectious recombinant baculoviruses by site-specific transposon-mediated insertion of foreign genes into a baculovirus genome propagated in *Escherichia coli*. J. Virol. **67:**4566–4579.
33. **O'Reilly DR, Miller LK, Luckow VA.** 1992. Baculovirus expression vectors: a laboratory manual. Oxford University Press, New York, NY.
34. **Wu W, Lin T, Pan L, Yu M, Li Z, Pang Y, Yang K.** 2006. *Autographa californica* multiple nucleopolyhedrovirus nucleocapsid assembly is interrupted upon deletion of the *38K* gene. J. Virol. **80:**11475–11485.
35. **Yuan M, Wu W, Liu C, Wang Y, Hu Z, Yang K, Pang Y.** 2008. A highly conserved baculovirus gene *p48* (*ac103*) is essential for BV production and ODV envelopment. Virology **379:**87–96.
36. **Cai Y, Long Z, Qiu J, Yuan M, Li G, Yang K.** 2012. An *ac34* deletion mutant of *Autographa californica* nucleopolyhedrovirus exhibits delayed late gene expression and a lack of virulence *in vivo*. J. Virol. **86:**10432–10443.
37. **Daimon T, Katsuma S, Iwanaga M, Kang W, Shimada T.** 2005. The *BmChi-h* gene, a bacterial-type chitinase gene of *Bombyx mori*, encodes a functional exochitinase that plays a role in the chitin degradation during the molting process. Insect Biochem. Mol. Biol. **35:**1112–1123.
38. **Li L, Li Z, Chen W, Pang Y.** 2007. Cloning, expression of *Autographa californica* nucleopolyhedrovirus *vp39* gene in *Escherichia coli* and preparation of its antibody. Biotechnology **17:**5–7.

39. **Wang P, Granados RR.** 2000. Calcofluor disrupts the midgut defense system in insects. Insect Biochem. Mol. Biol. **30:**135–143.
40. **Lu M, Swevers L, Iatrou K.** 1998. The *p95* gene of *Bombyx mori* nuclear polyhedrosis virus: temporal expression and functional properties. J. Virol. **72:**4789–4797.
41. **Akhtar A, Becker PB.** 2001. The histone H4 acetyltransferase MOF uses a C2HC zinc finger for substrate recognition. EMBO Rep. **2:**113–118.
42. **Klug A, Rhodes D.** 1987. Zinc fingers: a novel protein fold for nucleic acid recognition. Cold Spring Harbor Symp. Quant. Biol. **52:**473–482.
43. **Chen YR, Zhong S, Fei Z, Hashimoto Y, Xiang JZ, Zhang S, Blissard GW.** 2013. The transcriptome of the baculovirus *Autographa californica* multiple nucleopolyhedrovirus in *Trichoplusia ni* cells. J. Virol. **87:**6391–6405.
44. **Olszewski J, Miller LK.** 1997. Identification and characterization of a baculovirus structural protein, VP1054, required for nucleocapsid formation. J. Virol. **71:**5040–5050.
45. **Wang P, Granados RR.** 1997. An intestinal mucin is the target substrate for a baculovirus enhancin. Proc. Natl. Acad. Sci. U. S. A. **94:**6977–6982.
46. **Hou D, Zhang L, Deng F, Fang W, Wang R, Liu X, Guo L, Rayner S, Chen X, Wang H, Hu Z.** 2013. Comparative proteomics reveal fundamental structural and functional differences between the two progeny phenotypes of a baculovirus. J. Virol. **87:**829–839.
47. **Hong T, Summers MD, Braunagel SC.** 1997. N-terminal sequences from *Autographa californica* nuclear polyhedrosis virus envelope proteins ODV-E66 and ODV-E25 are sufficient to direct reporter proteins to the nuclear envelope, intranuclear microvesicles and the envelope of occlusion derived virus. Proc. Natl. Acad. Sci. U. S. A. **94:**4050–4055.
48. **Saksena S, Shao Y, Braunagel SC, Summers MD, Johnson AE.** 2004. Cotranslational integration and initial sorting at the endoplasmic reticulum translocon of proteins destined for the inner nuclear membrane. Proc. Natl. Acad. Sci. U. S. A. **101:**12537–12542.
49. **Braunagel SC, Williamson ST, Saksena S, Zhong Z, Russell WK, Russell DH, Summers MD.** 2004. Trafficking of ODV-E66 is mediated via a sorting motif and other viral proteins: facilitated trafficking to the inner nuclear membrane. Proc. Natl. Acad. Sci. U. S. A. **101:**8372–8377.
50. **Braunagel SC, Summers MD.** 2007. Molecular biology of the baculovirus occlusion-derived virus envelope. Curr. Drug Targets **8:**1084–1095.
51. **Song J, Wang R, Deng F, Wang H, Hu Z.** 2008. Functional studies of *per os* infectivity factors of *Helicoverpa armigera* single nucleocapsid nucleopolyhedrovirus. J. Gen. Virol. **89:**2331–2338.
52. **Elorza MV, Rico H, Sentandreu R.** 1983. Calcofluor white alters the assembly of chitin fibrils in *Saccharomyces cerevisiae* and *Candida albicans* cells. J. Gen. Microbiol. **129:**1577–1582.
53. **Eisemann CH, Donaldson RA, Pearson RD, Cadogan LC, Vuocolo T, Tellam RL.** 1994. Larvicidal activity of lectins on *Lucilia cuprina*: mechanism of action. Entomol. Exp. App. **72:**1–10.
54. **Harper MS, Hopkins TL, Czapla TH.** 1998. Effect of wheat germ agglutinin on formation and structure of the peritrophic membrane in European corn borer (*Ostrinia nubilalis*) larvae. Tissue Cell **30:**166–176.
55. **Wang P, Granados RR.** 2001. Molecular structure of the peritrophic membrane (PM): identification of potential PM target sites for insect control. Arch. Insect Biochem. Physiol. **47:**110–118.
56. **Vialard JE, Yuen L, Richardson CD.** 1990. Identification and characterization of a baculovirus occlusion body glycoprotein which resembles spheroidin, an entomopoxvirus protein. J. Virol. **64:**5804–5811.
57. **Cheng X, Krell P, Arif B.** 2001. P34.8 (GP37) is not essential for baculovirus replication. J. Gen. Virol. **82:**299–305.
58. **Wormleaton S, Kuzio J, Winstanley D.** 2003. The complete sequence of the *Adoxophyes orana* granulovirus genome. Virology **311:**350–365.
59. **Sternlicht MD, Lochter A, Sympson CJ, Huey B, Rougier JP, Gray JW, Pinkel D, Bissell MJ, Werb Z.** 1999. The stromal proteinase MMP3/stromelysin-1 promotes mammary carcinogenesis. Cell **98:**137–146.
60. **Ko R, Okano K, Maeda S.** 2000. Structural and functional analysis of the *Xestia c-nigrum* granulovirus matrix metalloproteinase. J. Virol. **74:**11240–11246.
61. **Volkman LE.** 2007. Baculovirus infectivity and the actin cytoskeleton. Curr. Drug Targets **8:**1075–1083.
62. **Uwo MF, Ui-Tei K, Park P, Takeda M.** 2002. Replacement of midgut epithelium in the greater wax moth, *Galleria mellonela*, during larval-pupal moult. Cell Tissue Res. **308:**319–331.
63. **Xiang X, Chen L, Hu X, Yu S, Yang R, Wu X.** 2011. *Autographa californica* multiple nucleopolyhedrovirus *odv-e66* is an essential gene required for oral infectivity. Virus Res. **158:**72–78.
64. **Sugiura N, Setoyama Y, Chiba M, Kimata K, Watanabe H.** 2011. Baculovirus envelope protein ODV-E66 is a novel chondroitinase with distinct substrate specificity. J. Biol. Chem. **286:**29026–29034.
65. **Kim JG, Hudson LD.** 1992. Novel member of the zinc finger superfamily: a C2-HC finger that recognizes a glia-specific gene. Mol. Cell. Biol. **12:**5632–5639.
66. **Peng K, van Oers MM, Hu Z, van Lent JW, Vlak JM.** 2010. Baculovirus *per os* infectivity factors form a complex on the surface of occlusion-derived virus. J. Virol. **84:**9497–9504.